Epitaxial growth and structure of $(La_{1-x}Lu_x)_2O_3$ alloys on Si(111)

T. Watahiki, F. Grosse,[a] W. Braun, V. M. Kaganer, A. Proessdorf, A. Trampert, and H. Riechert

Paul-Drude-Institut für Festkörperelektronik, Hausvogteiplatz 5-7, D-10117 Berlin, Germany

(Received 23 March 2010; accepted 15 June 2010; published online 21 July 2010)

$LaLuO_3$ layers are epitaxially grown on Si(111) by molecular beam epitaxy using high temperature effusion sources. Samples are prepared by simultaneous as well as alternating growth of La_2O_3 and Lu_2O_3. Grazing incidence x-ray diffraction indicates that the resulting crystal structure of the alloys is cubic. Simultaneous and alternating growth with a monolayer period lead to the same distribution of La and Lu with no preferential ordering. In all cases the lattice mismatch to Si is less than 0.6%. The experimental results are analyzed by studying the energetics of hexagonal, bixbyite, and perovskite $(La_{1-x}Lu_x)_2O_3$ crystal structures employing density functional theory. © *2010 American Institute of Physics*. [doi:10.1063/1.3460272]

The continuous scaling of Si CMOS devices requires the reduction in the thickness of the gate dielectric and leads to the replacement of conventional SiO_2 by high dielectric material such as Hf oxide. However, HfO_2 and its silicate have a dielectric constant (κ) of only 20 or less. Further scaling requires a higher κ value, band offsets to Si larger than 1 eV, and a higher thermal stability. Rare earth metal oxides, which include La_2O_3, Gd_2O_3, and Lu_2O_3,[1,2] are promising alternative high-κ gate dielectrics for future CMOS technology. Among them, $(La_{1-x}Lu_x)_2O_3$ has been proposed because of its large conduction band offset with Si and high reported κ value of about 32.[3] A critical issue for implementation in devices is the interface formation to Si and, related to it, a low defect density. A possible route is a lattice matched growth on Si. The appropriate mixture of La_2O_3, which has a lattice parameter approximately 4% larger than Si, and Lu_2O_3, with a 4% smaller lattice parameter than Si, allows to achieve this goal, as it will be demonstrated in this article. On the other hand, mixing two materials with a deviation of the lattice parameters by 8% results in large internal strain and might cause phase separation.[4]

In this paper, we study the epitaxial growth of $(La_{1-x}Lu_x)_2O_3$ on Si(111) by molecular beam epitaxy (MBE) with concentrations close to $x=0.5$, which will be abbreviated in the following by $LaLuO_3$. High temperature effusion cells have been especially designed to evaporate each La_2O_3 and Lu_2O_3 materials from the Ta crucible with temperature control. Compared to an e-beam evaporator, this source allows a very precise flux control. During oxide growth, molecular oxygen gas was introduced into the chamber through a nozzle in a source port location with a typical partial pressure of $0.6–1.0\times10^{-7}$ mbar. The growth is monitored by reflection high-energy electron diffraction (RHEED) in order to investigate the layering during growth by observing the specular spot oscillations. After growth, the samples are transferred in a vacuum shuttle (to avoid reaction with air) to the chamber for measuring grazing incidence x-ray diffraction (GIXRD). GIXRD measurements are performed with 10 keV synchrotron radiation at the PHARAO beamline (U125/2-KMC) at BESSY, Berlin, Germany.[5] The XRD measurements on the Si(111) substrate are described within the hexagonal coordinate system.[6] To avoid confusion with cubic coordinates, the suffix "hex" is added when we use the Miller indices for the hexagonal system.

Figure 1(a) shows the intensity evolution of the specular spot in RHEED during the growth of the digital $LaLuO_3$ alloy. The growth rates, obtained from RHEED oscillations, are around 1 monolayer (ML) in 80 s and 120 s correspond-

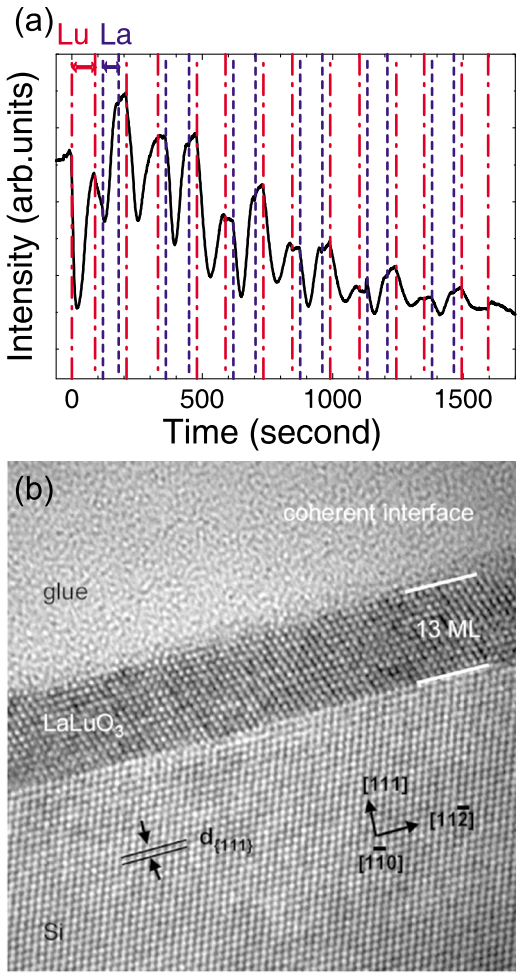

FIG. 1. (Color online) (a) Intensity evolution of the specular spot in RHEED during the deposition of the digitally-grown $LaLuO_3$ alloy. (b) High resolution TEM image of the digitally grown layer.

[a]Electronic mail: frank.grosse@pdi-berlin.de.

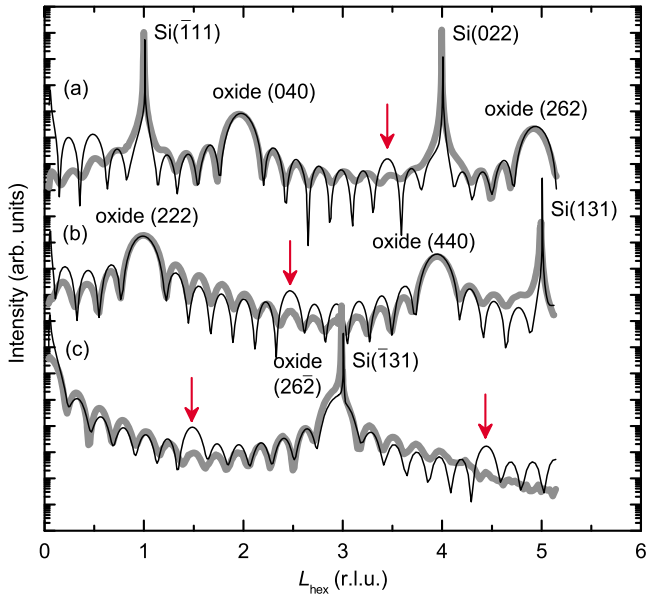

FIG. 2. (Color online) CTRs (a) $(10L)_{hex}$, (b) $(1\bar{1}L)_{hex}$, and (c) $(2\bar{1}L)_{hex}$ for the digitally grown oxide layer compared with simulated curves. The measured data are shown by bold gray lines. Black curves represent the simulations for the 180° rotated cubic phase. Positions of additional peaks expected due to the double periodicity of the digital alloy are shown by arrows.

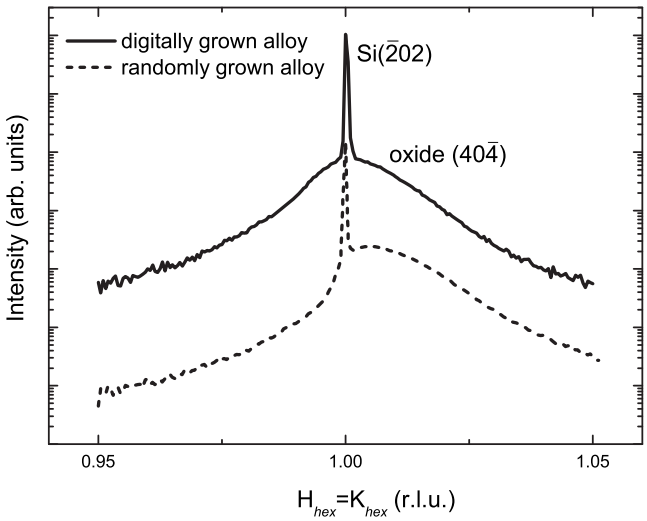

FIG. 3. GIXRD pattern around in-plane Si(2̄02) reflection for (a) digitally grown alloy and (b) uniform alloy.

ing to the cell temperature readings of 1650 °C and 1850 °C for La_2O_3 and Lu_2O_3, respectively. The typical specular spot RHEED oscillations indicate good layering of $LaLuO_3$ on Si(111). The initial layer is chosen to be Lu_2O_3. We design to grow 1 ML of Lu_2O_3 and La_2O_3 alternatively by shutter control with observing RHEED oscillation until the film reaches a total thickness of 13 ML. The last layer is Lu_2O_3.

As a comparison, we also have grown an $LaLuO_3$ alloy by opening both shutters of La_2O_3 and Lu_2O_3 simultaneously (randomly grown alloy). In this case, we adjust the flux of each oxide by choosing corresponding effusion cell temperatures resulting in identical growth rates of 1 ML per 80 s. The grown layer is 14 ML thick, confirmed by x-ray reflectivity measurement. Figure 1(b) shows the transmission electron microscopy (TEM) image of the digitally grown sample. It reveals that the oxide/Si interface is abrupt. Silicate formation is not observed. Also, the layer thickness is almost uniform and is approximately 13 ML, which agrees perfectly with the thickness deduced from specular spot RHEED oscillations. This result indicates a very precise flux control in our growth experiment by using high temperature effusion sources. Additionally, no threading dislocations are observed, evidencing a coherent growth.

We studied the structure of the epitaxial $LaLuO_3$ layer by XRD. There are several $LaLuO_3$ structures reported. While single crystal $LaLuO_3$ and epitaxial $LaLuO_3$ layers grown on $SrTiO_3$ have perovskite (orthorhombic) structure,[7,8] the hexagonal structure is reported for epitaxially grown $LaLuO_3$ grown on Si(111).[9] According to the phase diagram, La_2O_3 and Lu_2O_3 should be stable in hexagonal and cubic bixbiyte phase, respectively, at a substrate temperature of 700 °C.[10]

Figure 2 compares crystal truncation rods (CTRs) $(10L)_{hex}$, $(1\bar{1}L)_{hex}$, and $(2\bar{1}L)_{hex}$ for the digitally grown layer with simulated curves. The CTRs indicate that the structure of this layer is cubic, not hexagonal nor orthorhombic. The $LaLuO_3(111)$ layer normal is parallel to the Si(111) substrate normal with the oxide layer 180° rotated in-plane with respect to Si substrate, similar to other rare earth oxides like Gd_2O_3 (Ref. 11) and Pr_2O_3.[12]

There are no detectable twins that could be caused by the coexistence of rotated (B-type) and nonrotated (A-type) domains. The fact that the interference fringes do not vanish between the reflections, evidences the good thickness uniformity of the films. A thickness variation approaching or exceeding half a ML or more would lead to a damping of the oscillations at the antiphase point between the allowed reflections. The fact that fringes are not extinct at this point means that the film is uniform to within less than 0.5 ML over several square millimetre sampled by the XRD experiment.

The diffraction peaks which are expected to appear, due to the double periodicity of a nominally digitally grown layer, between the layer peaks, are missing in the measured CTRs. They clearly appear in the calculated CTRs for a digital layer and are marked in Fig. 2 by arrows. The CTRs for randomly grown alloy layer (not shown here) also reveal a similar diffraction pattern. This means that the intended alternating layer sequence La_2O_3/Lu_2O_3 in the digitally grown layer is lost.

Figure 3 shows the GIXRD pattern around the in-plane reflection Si(2̄02). The in-plane lattice constant of the digitally grown layer is found to be only 0.2% smaller than that of Si while the uniform alloyed layer has a 0.5%–0.6% mismatch to Si. This difference is probably due to a deviation in the flux adjustment of the two MBE sources. Therefore, rare-earth oxide layers with exact lattice matching to Si and without dislocations at the interface can be grown by adjusting the composition ratio of La/Lu and controlling the growth methods.

Owing to the abrupt interface, we can precisely analyze the vertical position of the oxide layer on Si(111). By fitting the CTRs, we find the distance between top Si atoms and the lowest plane of rare earth metal atoms as 0.25 ± 0.01 nm, which corresponds to the bond length of 0.14–0.2 nm between bottom oxygen and top Si atoms, see Fig. 4. It agrees

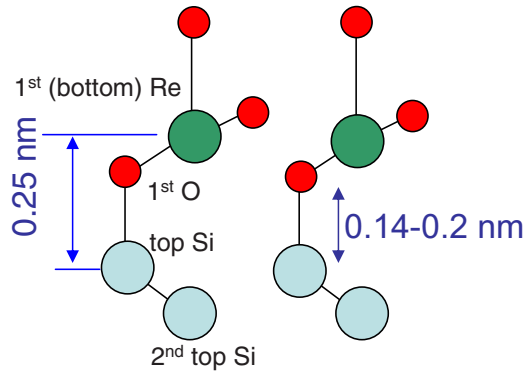

FIG. 4. (Color online) The interface between the rare-earth oxide layer and Si(111).

well with the sum of the covalent radii of Si and O, which are 0.11 nm and 0.7 nm, respectively.

The experimental findings are supported by calculations employing density functional theory (DFT) (Refs. 13 and 14) treating the exchange-correlation part by local density approximation (LDA)+U (Ref. 15) within the projected augmented plane wave method. Further computational details can be found elsewhere.[16] The calculated structural data of the binary compounds La_2O_3 and Lu_2O_3 agree very well with experimental values. The stable crystal structure is correctly given for La_2O_3 to be hexagonal and for Lu_2O_3 bixbyite. Based on these results for the binary constituents, different $(La_{1-x}Lu_x)_2O_3$ unit cells were constructed which differ in concentration x, local arrangement of the rare earth metal atoms La and Lu, and average crystal structure (hexagonal and bixbyite). The formation enthalpy $\Delta H = E_{\mathrm{tot}} - (1-x)E_{\mathrm{tot}}^{La_2O_3} - xE_{\mathrm{tot}}^{Lu_2O_3}$ is calculated with respect to the stable phases of La_2O_3 and Lu_2O_3. The numerical values are given in Fig. 5. Low formation enthalpies are found for the hexagonal structures at low Lu_2O_3 concentration whereas at higher concentration cubic structures are more favorable. At $x=0.5$ lowest formation enthalpy is found for the perovskite crystal structure. Structures with a digital layering, i.e., alternating La_2O_3 and Lu_2O_3 layers along the hexagonal [0001] direction, exhibit large formation enthalpies. Therefore, there is a tendency for intermixing of La and Lu layers to reduce the energy as observed in the growth experiments.

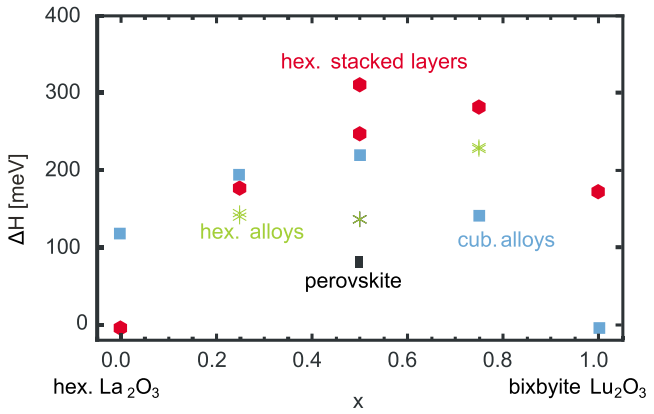

FIG. 5. (Color online) Formation enthalpy ΔH for various ordered structures with respect to hexagonal La_2O_3 and cubic (bixbyite) Lu_2O_3. Filled hexagons: layered hexagonal La_2O_3/Lu_2O_3 digital [0001] alloys; stars: hexagonal mixed structures; filled squares: mixed cubic (bixbyite) structures; rectangle: perovskite $LaLuO_3$.

Despite the high structural quality, preliminary measurements of the electrical properties did not show significant improvements over previous results.[7] A more quantitative investigation especially with respect to the oxygen distribution is necessary to clarify the seemingly disconnected relation between structural and electrical results.

In summary, we fabricated digitally and randomly grown $LaLuO_3$ alloys to investigate the differences in their structures. XRD measurements show that $LaLuO_3$ grown on Si(111) has a cubic structure. Detailed measurements reveal that the digitally grown $LaLuO_3$ alloy has a very small lattice mismatch of 0.2% with respect to that of Si and a compressive strain in in-plane direction, while the randomly grown alloy has a mismatch of 0.5%–0.6% with a nearly relaxed layer. The formation enthalpies calculated by DFT show that digital layers have high values. The observed alloying of the constituents is therefore an equilibration effect.

We thank S. Behnke for the support of the experiments and R. Hey for the critical reading of the manuscript. This work was supported by the German Federal Ministry of Education and Research through the project MEGAEPOS.

[1] T. Hattori, T. Yoshida, T. Shiraishi, K. Takahashi, H. Nohira, S. Joumori, K. Nakajima, M. Suzuki, K. Kimura, I. Kashiwagi, C. Ohshima, S. Ohmi, and H. Iwai, Microelectron. Eng. **72**, 283 (2004).
[2] M. Czernohorsky, E. Bugiel, H. Osten, A. Fissel, and O. Kirfel, Appl. Phys. Lett. **88**, 152905 (2006).
[3] J. M. J. Lopes, M. Roeckerath, T. Heeg, E. Rije, J. Schubert, S. Mantl, V. V. Afanas'ev, S. Shamuilia, A. Stesmans, Y. Jia, and D. G. Schlom, Appl. Phys. Lett. **89**, 222902 (2006).
[4] O. Rubel, K. Volz, T. Torunski, S. Baranovskii, F. Grosse, and W. Stolz, Appl. Phys. Lett. **85**, 5908 (2004).
[5] B. Jenichen, W. Braun, V. Kaganer, A. Shtukenberg, L. Däweritz, C. Schulz, K. Ploog, and A. Erko, Rev. Sci. Instrum. **74**, 1267 (2003).
[6] G. Grübel, K. G. Huang, D. Gibbs, D. M. Zehner, A. R. Sandy, and S. G. J. Mochrie, Phys. Rev. B **48**, 18119 (1993).
[7] J. Schubert, O. Trithaveesak, W. Zander, M. Roeckerath, T. Heeg, H. Y. Chen, C. L. Jia, P. Meuffels, Y. Jia, and D. G. Schlom, Appl. Phys. A: Mater. Sci. Process. **90**, 577 (2008).
[8] K. L. Ovanesyan, A. G. Petrosyan, G. O. Shirinyan, C. Pedrini, and L. Zhang, Opt. Mater. **10**, 291 (1998).
[9] V. V. Afanas'ev, M. Badylevich, A. Stesmans, A. Laha, H. J. Osten, A. Fissel, W. Tian, L. F. Edge, and D. G. Schlom, Appl. Phys. Lett. **93**, 192105 (2008).
[10] G. Adachi and N. Imanaka, Chem. Rev. **98**, 1479 (1998).
[11] A. Fissel, D. Kühne, E. Bugiel, and H. J. Osten, Appl. Phys. Lett. **88**, 153105 (2006).
[12] T. Schroeder, P. Zaumseil, G. Weidner, C. Wenger, J. Dabrowski, H.-J. Mussig, and P. Storck, J. Appl. Phys. **99**, 014101 (2006).
[13] X. Gonze, J.-M. Beuken, R. Caracas, F. Detraux, M. Fuchs, G.-M. Rignanese, L. Sindic, M. Verstraete, G. Zerah, F. Jollet, M. Torrent, A. Roy, M. Mikami, Ph. Ghosez, J. Y. Raty, and D. C. Allen, Comput. Mater. Sci. **25**, 478 (2002).
[14] X. Gonze, G.-M. Rignanese, M. Verstraete, J.-M. Beuken, Y. Pouillon, R. Caracas, F. Jollet, M. Torrent, G. Zerah, M. Mikami, Ph. Ghosez, M. Veithen, J.-Y. Raty, V. Olevano, F. Bruneval, L. Reining, R. Godby, G. Onida, D. R. Hamann, and D. C. Allan, Z. Kristallogr. **220**, 558 (2005).
[15] B. Amadon, F. Jollet, and M. Torrent, Phys. Rev. B **77**, 155104 (2008).
[16] F. Grosse, T. Watahiki, and W. Braun, Thin Solid Films **518**, 4747 (2010).